

Performance of the position sensitive photodetector with early stage digitizing of the photocurrents

J. M. ELAZAR, S. J. PETRICEVIC

School of Electrical Engineering, University of Belgrade, Bulevar Kralja Aleksandra 73, Serbia

Analog circuits processing PSD currents and calculating position value introduce errors of significant magnitude and demand separate circuits for amplitude and phase detection methods, thus prohibiting full use of the PSD's potential. In order to demonstrate PSD capabilities, a high performance electronics circuit has been constructed that digitizes PSD photocurrents and calculates position value using DFT from both amplitude and phase methods. Verification of the total system error has been independently carried out using Michelson interferometer. Comparison of both detection methods offers better insight into their potential use. Experimental results qualify PSD as detector capable of 100 nm displacement resolution in direct illumination setup.

(Received December 12, 2011; accepted February 20, 2012)

Keywords: Position sensitive detector, Optical position measurement, Photocurrent digitizing, PSD linearity, PSD position detection error

1. Introduction

PSD has long been used as a position sensitive optical detector for measuring position, range, speed, and other quantities. PSD models have been accurately defined in both frequency and time domain [1,2,3,4,5], and as such have provided the ground required for introducing the carrier in the probing light [5,6] as a method for system performance improvement. However, analog electronic processing technology introduces errors in position detection process, primarily because of the difficulty of performing division, which directly influences system level linearity, and of course, additional noise caused by complicated signal processing circuitry. These issues have led to various workarounds, including developments of a new method for light spot position determination [5,6] and processing PSD photocurrents in the digital domain [7]. Thorough examination of the noise in a PSD system [8] has proved that post-PSD electronic processing circuit has detrimental effect on the total system performance. Introduction of the audio frequency range IC AD converters capable of 20 bits+ resolution at sample rates of 50 KSPS and more, presents designers with an opportunity for early stage PSD photocurrent analog to digital conversion. Once converted, signal is processed in the digital domain, thus eliminating all errors resulting from inadequate analog processing circuits. It is also possible to correct system level nonlinearities by means of calibration and lookup table.

Recent work [9, 10] demonstrates advances in the field with micrometer resolution of detection. Further improvements can be achieved by amplitude modulation of

the light carrier and later processing in the frequency domain [11].

The purpose of this paper is to demonstrate capabilities of the PSD in its primary role, by means of inclusion of the carrier modulated light, high performance electronic processing circuitry and digital signal processing using DFT. In order to verify performance an independent position sensing system has been constructed for the purpose of testing and calibration. Ultimate resolution of 100 nm in direct position detection has been demonstrated within the range of 5 mm (roughly 16 bits of dynamic range).

2. The model

PSD frequency domain model is required in order to perform proposed measurements. Assuming reverse bias, negligible light spot size and disregarding input impedance of the transimpedance amplifier, equations describing instantaneous value of the photocurrents at the left and right PSD electrode when the PSD is excited with sinusoidal modulated light are [6]

$$\begin{aligned} i_L &= I_0 \operatorname{Re} \left[\frac{\operatorname{Sinh}[\gamma(L-x_1)]}{\operatorname{Sinh}(\gamma L)} \right] e^{j\omega t} \\ i_R &= I_0 \operatorname{Re} \left[\frac{\operatorname{Sinh}[\gamma x_1]}{\operatorname{Sinh}(\gamma L)} \right] e^{j\omega t} \end{aligned} \quad (1)$$

where ω is the light carrier frequency, L is the PSD active

area dimension, x_1 is the location of the light spot, I_0 is total PSD photocurrent. Constant γ is generally referred to as propagation constant (since PSD electrical model is a distributed network) whose value is dependent on the electrical characteristics of the PSD, i.e. it's resistance and capacitance.

Due to non linear nature these equations have been subjected to two important approximations. First, for typical values of the PSD model's electrical parameters the product γx_1 is sufficiently small to disregard all but the first term in the Taylor series expansion of the Eq. (1), leading to equations for photocurrent phasor amplitudes

$$\begin{aligned} I_L &\approx I_0 \frac{L - x_1}{L} \\ I_R &\approx I_0 \frac{x_1}{L} \end{aligned} \quad (2)$$

Solving for x_1 requires knowledge of both photocurrents or one of the two electrode photocurrent and common electrode photocurrent. Since measuring I_0 complicates somewhat transimpedance amplifier if PSD is to be inversely polarized, and since modulated light source of highly stable amplitude is difficult to realize, Eq. (2) is conveniently solved as

$$x_1 = \frac{L}{2} \left(1 - \frac{I_L - I_R}{I_L + I_R} \right) \quad (3)$$

Eq. (3) is usually referred to as the normalized position equation since it does not require I_0 to be measured although it does use the sum of the photocurrents to normalize position value to the total photocurrent, thus eliminating influence of the light source power instability. This equation models the amplitude detection method returning values for light spot position x_1 in the range $[0, L]$.

Second approximation involves expanding $\sinh()$ function [6]

$$dP = \phi - \theta = \frac{2\omega RCL}{\pi^2} \left(x_1 - \frac{L}{2} \right) \sum_{n=1}^{\infty} \frac{1}{n^2} \quad (4)$$

The difference in phase of the photocurrent phasors can be used to measure light spot position x_1 and is the basis of the phase detection method. However, this method is much less linear than amplitude method, particularly near PSD edges.

3. Experiment preparation

In order to conduct proposed experiment, it was necessary to devise two auxiliary functional blocks under

the command of the personal computer. This is required in order to make automatic measurement and to acquire data with adequate speed since measurements will be conducted with several thousand measuring points. Testing entire PSD active area and attaining adequate resolution requires that the PSD to be mounted on a mechanized single axis positioner driven by a stepper motor. Since nominal step of the positioner was declared by the manufacturer to be 20 μm , we have constructed a micro stepping electronic driver capable of driving the carrier platform with 10 nm steps.

Step deviations and position error of the motorized positioner require that an independent position detection device be used for calibration. To satisfy high resolution demands and having in mind small scan area (typical 1D PSD dimensions are in the order of few millimeters), a mirror in the sensing arm of the Michelson interferometer was coupled to the movable platform, thus measuring the position of the platform with sufficient accuracy. Detection of the interferometer fringes was conducted by a large area CCD device with 1024 pixel on a 10mm length. This device outputs standard video signal representing the distribution of the light intensity across interference fringes. Interferometer's image was projected on the CCD active area by a lens that expanded fringes for better resolution and setting an integer number of fringes on the CCD active area. This is useful for later signal processing in order to obtain accurate position from the interferometer. Both devices have been placed under the control of the PC that was driving the platform with a high resolution and interpreting the images from the interferometer. Motion of the fringes is related in a linear way to the platform motion. In order to calculate platform displacement (interferometer is an incremental device), an FFT on the fringe's image was conducted. Since integer number of fringes were placed on an CCD area, it was easy to separate dominant frequency related to the integer number of fringes on a CCD scan area and obtain it's phase shift. Subtracting phase shifts and multiplying by predetermined quotient gives platform displacement.

Having created necessary test conditions, entire system was tested without PSD. Noise in interferometer sensed position was tested with intention to determine minimal discernable platform displacement. A total of 10 000 samples were taken with steady platform position (positioner stepper motor windings powered with constant currents) and it was found that displacement values followed normal distribution. Thus, mean displacement value of -0.03 nm and deviation of 1nm were calculated, indicating a r.m.s. noise in displacement of 1nm and negligible drift.

4. High performance electronic detection circuit

Testing capabilities of an analog sensor (potentially an unlimited resolution device) placed more than stringent demands on the design and manufacturing of an electronic

detection circuit with purpose was of amplifying and measuring PSD photocurrents. PSD photocurrents should be digitized immediately following the primary transimpedance amplifier stage with a high resolution, high linearity AD converter. A PC carried out signal processing in digital domain, allowing testing of both detection methods. This circuit also generates sinusoidal signal of controllable frequency and low noise amplitude for the purpose of light source modulation (the carrier).

Primary transimpedance stage was conceived around OPA655, a high performance JFET op-amp, performing a task of photocurrent amplification and conversion to voltage. This stage was caged inside a metal box in order to shield sensitive high impedance nodes from EM interference. Once converted and amplified signal currents are presented to the CS4222 audio codec, an IC stereo AD-DA converter. Each photocurrent is digitized by one channel with 20bits at 50KSPS. The same printed circuit board includes an EPROM with digital representation of the sinusoidal waveform that fed the DA to generate distortion clean and high stability amplitude carrier. This mixed signal circuit was decoupled from the PC by optocouplers and a FIFO interface circuit. Time series from AD converters was analyzed by DFT, and amplitude and phase of the frequency component representing the carrier were used to calculate position using both methods. Isolating sensitive analog circuit from the PC and powering from batteries, resulting in best possible performance. Since two independent channels are used, automatic calibration takes places before actual measurement and proper calibration quotients for amplitude and phase are used in calculus to normalize signal values.

In order to verify performance of the electronic detection circuit a loop back test was carried to determine noise level. Output from DA converter that will modulate light source was fed directly to both AD converter channels. Measurements of noise in both channels as well as in position calculated from those values were carried out using this setup. Noise in signal current amplitude amounts to 1ppm, as is the noise in position value calculated by amplitude method.

5. Experimental setup

Block diagram of the experiment setup is depicted in Fig. 1.

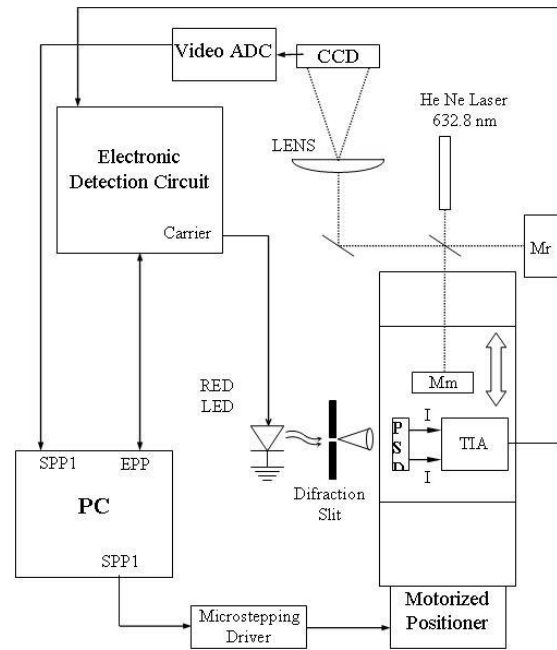


Fig. 1. Experiment setup.

All mechanical and optical components in the experiment were mounted on an optical bench insuring firm placement. Center point of the setup is the moving platform mounted on the motorized stage. It carries the PSD and primary transimpedance stage (TIA) shielded in a box and the mirror of the measuring arm of the Michelson interferometer (Mm). Interferometer light source is a HeNe laser operating at 632.8 nm at 1 mW CW power. Beam splitter divides source beam into two arms (reference arm mirror denoted Mr). In order to enlarge fringe picture projected on the CCD, both beams are projected through a lens. Fringes are captured by the CCD and transferred to a video AD converter to the PC's parallel port (denoted SPP1). Image is processed using FFT and phase of the fringes calculated, from which displacement of the platform is derived. Platform position is set by microstepping stage controlled by PC's parallel port (SPP2). Electronic detection circuit is linked to a PC by an EPP bi-directional parallel port enabling commands from and data to PC. PC controls carrier frequency and amplitude, which drives high brightness red LED. Light beam from LED was projected on a vertical variable diffraction slit in close contact with PSD. This arrangement produces stable vertical line spot of controllable width thus enabling us to test effect of light spot size on the PSD performance. Platform moved the PSD across the diffraction slit thus effecting active area scan. Amplitude modulated PSD photocurrents signals are fed to the electronic detection circuit where amplification and AD conversion takes place. Time series is transferred to the PC's main memory for signal processing. DFT extracts amplitude and phase information that is used to calculate digital position value by both methods.

In order to verify test spot shape a linear CCD array was placed at the PSD position and spot shapes recorded by an oscilloscope. Results are presented in Fig. 2. Spot sizes were measured using FWHM (full width at half magnitude) criterion.

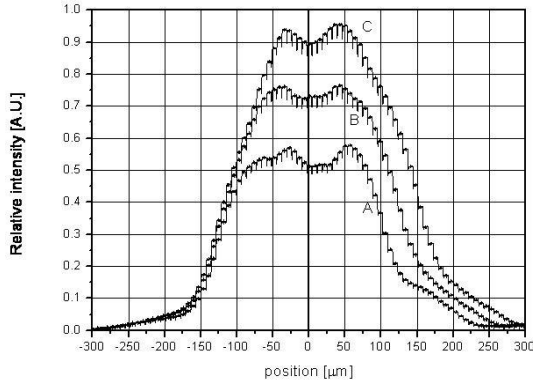


Fig. 2. CCD line scan of the PSD test spot transverse profiles.

Three spot sizes used to test PSD have been named for convenience as A, B and C spots.

Table 1. Spot sizes.

Slit position (spot size)	FWHM
A	232
B	245
C	254

Custom program written in C language controlled the experiment. It was charged with positioning the platform, reading interferometer image and determining platform position, acquiring PSD photocurrent values and performing necessary signal processing to determine PSD sensed position.

6. Experimental results

Unless otherwise noted, following statements are valid for all graphs:

PSD used is SiTek 1L5 with following electrical characteristics:

PSD Length 5mm

Total PSD resistance 50K \square (typ.)

PSD capacitance 6pF

Carrier frequency is 187.5Hz.

Light spot is A size, modulation depth 90%.

Graphs are normalized with respect to PSD electrical center.

Fig. 3 depicts normalized PSD photocurrents amplitude when scanned across entire active area. This

graph reveals not only functional form of the PSD photocurrents given by Eq. (2) but also demonstrates edge effects. First, closing on one electrode, total photocurrent which is linearly related to light spot intensity, drops, indicating diffraction losses at the edge. Abrupt signal loss very close to the PSD edge is of course caused by the inability of the transimpedance stage to provide zero impedance input. This action takes place when output resistance of the electrode to which the light spot is moving becomes comparable to the input resistance of the transimpedance stage.

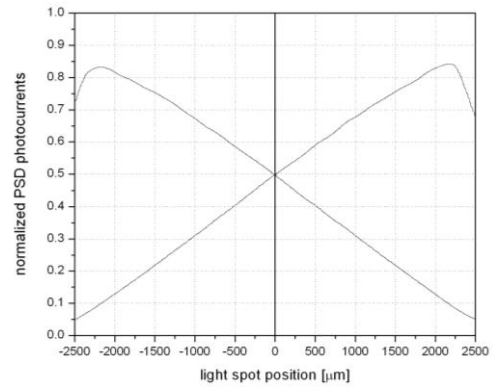


Fig. 3. Amplitudes of PSD photocurrents.

Changing spot size dimension reveals possible imperfections that could arise from the optical part of the system. Sweeping the spot from edge to edge as in Fig. 4. total PSD photocurrent does not depend in its form on light spot dimension variations, indicating that PSD glass window imperfections, dirt or grease, and of course, PSD layer nonlinearities, cause total photocurrent dependence on the spot position far from PSD edges. Had this been caused by variations in the slit diffraction pattern, curves would have been different for different spot sizes. This conclusion is in agreement with curves in Fig. 2. Sharp drop in magnitude at $\pm 2000\mu\text{m}$ confirms previous conclusions regarding influence of the transimpedance stage.

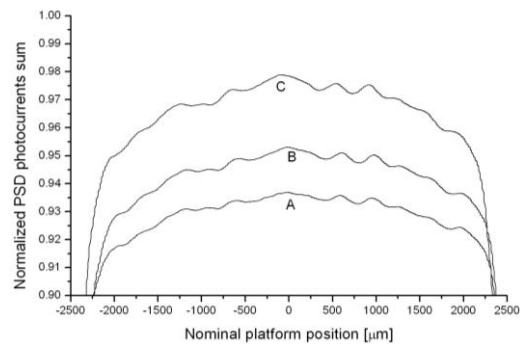


Fig. 4. Normalized sum of the PSD photocurrents over PSD active area with spot size as parameter.

The effect of position normalization due to dividing current difference with their sum, thus eliminating

influence of the light spot intensity, becomes visible at Fig. 5. This inherent quality of the amplitude method shall be augmented by good noise performance, thus lending itself to high performance position sensing. Changing light spot size did not influence PSD transfer function.

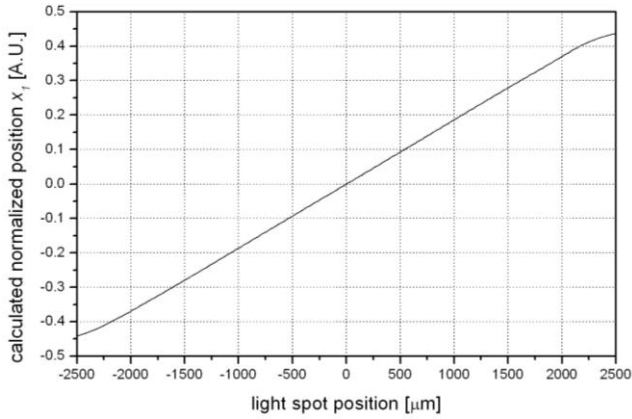


Fig. 5. Normalized position value x_I obtained by amplitude method.

Fig. 6 demonstrates difference in phases of the PSD photocurrents when the A spot size is swept from edge to edge. Linearity around electrical center, sensitivity variations with carrier frequency and asymmetry caused by asymmetrical light spot intensity in the transverse direction [12] are all clearly visible. Greater nonlinearity of this method near PSD edges is also visible. Since phase difference sensitivity varies with carrier frequency as found in [6] this function is plotted in Fig. 7. Increasing modulation frequency provides greater sensitivity but is limited by the bandwidth of the transimpedance stages.

In-depth analysis of the noise performance of the PSD-transimpedance stage combination can be found in [8]. Depending on the intensity of the light spot and thus the value of required transimpedance resistor, dominant noise source can be either light source noise, transimpedance stage operational amplifier voltage noise multiplied by noise gain or transimpedance resistor (also influencing noise gain). Without considering many possible combinations of dominant noise source and total noise magnitude, experimental results of the noise in the position value x_I were obtained as σ value from distribution of x_I (amplitude method) with fixed PSD position. Results are presented in Fig. 8. Noise floor of 20 ppm (normalized x_I span is 1) offers resolution of 100 nm with 5 mm sized PSD.

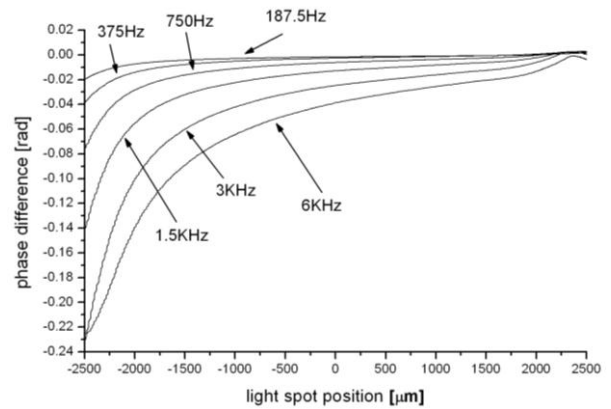


Fig. 6. Photocurrents phase difference with carrier frequency as a parameter.

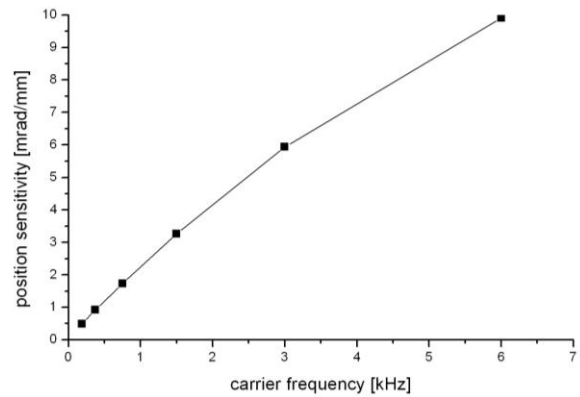


Fig. 7. Phase method sensitivity as a function of carrier frequency.

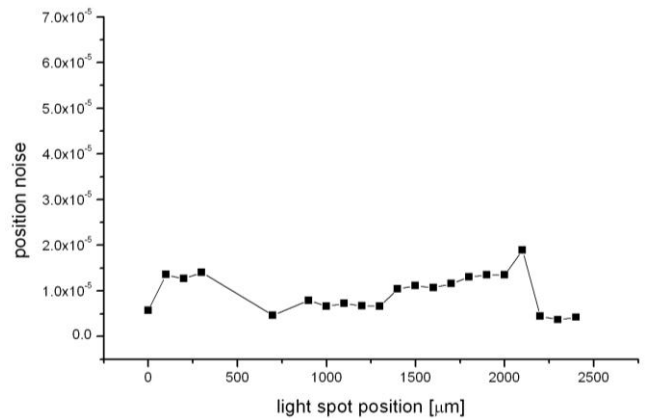


Fig. 8. Position noise (amplitude method) as a function of light spot position.

Having verified desired system level performance, we have tested PSD accuracy by comparing position obtained with Michelson interferometer and PSD sensed position (amplitude method). Results of light spot scan of 10 μm of the PSD area from its electrical center towards one electrode are presented in Fig. 9. Curves are deliberately made to have a 20 nm offset for the sake of clarity. Obviously, PSD sensed value follows closely true position

with same functional dependence caused by positioning error in motorized stage, thus indicating good linearity. Subtracting values offers insight into absolute position error, which is plotted in Fig. 10. Noise and remaining nonlinearity within this margin are difficult to discern.

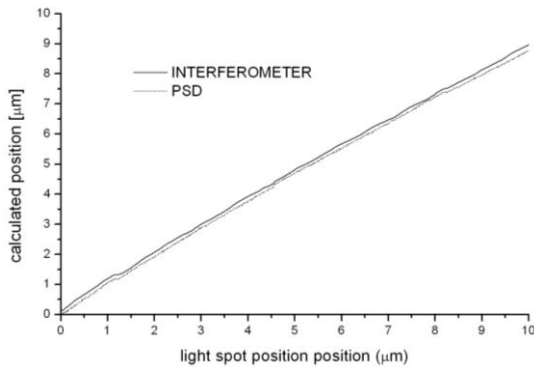


Fig. 9. Comparison of interferometer and PSD sensed position value.

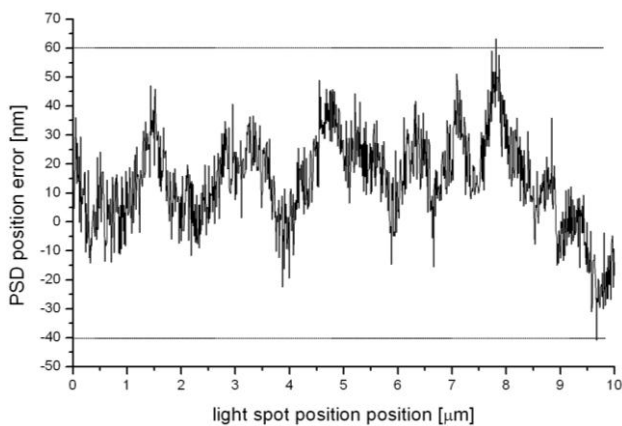


Fig. 10. PSD sensed position error.

7. Conclusion

In order to test ultimate PSD performance an early stage AD conversion on the PSD photocurrents using $\Sigma\Delta$ AD conversion technology and DFT processing of the PSD modulated carrier has been proposed. This position determination system provides optimal system level performance with the ability to correct system level errors with look up tables and enables both position detection methods to be used at the same time. Experiment involving variations in light spot size, carrier frequency and PSD active area scan offer detailed insight into PSD behavior. Theoretical results previously obtained are verified by experimental results. PSD linearity has been tested by comparing PSD sensed position values with Michelson interferometer and good linearity was found. Of particular importance is low system level noise in position value $\times 1$ of only 100 nm with 5 mm PSD, thus allowing the PSD to be used as a sub micrometer sensor.

References

- [1] K. Dutta, Y. Hatanaka, Solid State Electron. **32**, 485 (1989).
- [2] W. P. Connors, IEEE Trans. Electron Devices **8** (1971).
- [3] Lucovsky, Photo-effects in non-uniformly irradiated p-n junctions, J. Appl. Phys. **31** (1960).
- [4] J. Torkel Wallmark, Proc. IRE (1957).
- [5] C. Narayanan, A. Bruce Buckman, I. Busch-Vishniac, IEEE Trans. Instrum. Meas. **43**, 830 (1994).
- [6] Narayanan, A. Bruce Buckman, I. Busch-Vishniac, M. F. Becker, R. W. Bene, R. M. Walser, SPIE Smart Sensing, Processing, and Instrumentation **1918**, 205 (1993).
- [7] P. Schaefer, R. D. Williams, G. K. Davis, R. A. Ross, IEEE Trans. Instrum. Meas. **47**, 914 (1998).
- [8] C. Narayanan, A. B. Buckman, I. Busch-Vishniac, IEEE Trans. Instrum. Meas. **46**, 1137 (1997).
- [9] H. Liu, Y. Xiao, Z. Chen, IFCSTA 2009 Proceedings - 2009 International Forum on Computer Science-Technology and Applications **3**, 90 (2009).
- [10] X. He, Y. Zhong, X. Wang, H. Zheng, Research on position detection of PSD based on light intensity modulation and digital fit Proceedings of the 2009 WRI Global Congress on Intelligent Systems **3**, 38 (2009).
- [11] J. La, K. Park, Review of Scientific Instruments, **76**, 1 (2005).
- [12] H. Yuan, A. He, Z. Li, Z. Wang, Microwave Opt. Technol. Lett. **24**, 40 (2000).

*Corresponding author: slobodan@etf.rs